Study on Photoluminescence Quenching and Photostability Enhancement of MEH-PPV by Reduced Graphene Oxide

ARTICLE *in* THE JOURNAL OF PHYSICAL CHEMISTRY C · OCTOBER 2012

Impact Factor: 4.77 · DOI: 10.1021/jp306631y

8 AUTHORS, INCLUDING:

Chenxin Ran
Xi'an Jiaotong University
18 PUBLICATIONS **118** CITATIONS
SEE PROFILE

Minqiang Wang
Xi'an Jiaotong University
91 PUBLICATIONS **643** CITATIONS
SEE PROFILE

Xiaohui Song
Xi'an Jiaotong University
27 PUBLICATIONS **225** CITATIONS
SEE PROFILE

THE JOURNAL OF PHYSICAL CHEMISTRY C

Article

pubs.acs.org/JPCC

Study on Photoluminescence Quenching and Photostability Enhancement of MEH-PPV by Reduced Graphene Oxide

Chenxin Ran,[†] Minqiang Wang,*[,†] Weiyin Gao,[†] Jijun Ding,[†] Yanhua Shi,[†] Xiaohui Song,[†] Haowei Chen,[‡] and Zhaoyu Ren[‡]

[†]Electronic Materials Research Laboratory, Key Laboratory of Education Ministry, Xi'an Jiaotong University, Xi'an, Shaanxi 710049, P.R. China

[‡]Institute of Photonics and Photo-Technology, Provincial Key Laboratory of Photoelectronic Technology, Northwest University, Xi'an, Shaanxi 710069, P.R. China

ABSTRACT: In conjugated polymer based photovoltaic devices, efficient charge transfer and photostability of the fluorescence polymer are two essential properties, which could be responsible for better performance and longer lifetime of the device. Hence, it is of great importance to explore strategies that can enhance the exciton separation and improve the photostability of polymers. In this work, composites of poly[2-methoxy-5-(2-ethylhexyloxy)-1,4-phenylenevinylene] (MEH-PPV) participated by appropriate amounts of reduced graphene oxide (r-GO), which leads to a significant photoluminescence quenching as well as superior photostability of MEH-PPV, have been investigated. The photoluminescence quenching and photostability of MEH-PPV/r-GO composites have been observed by UV−visible and fluorescence spectroscopy. From transient fluorescence spectrum, the mechanism of photoluminescence quenching has been confirmed to be static quenching, which is caused by electron transfer at the interface of the composite. Furthermore, we propose that this very efficient photoinduced excitation electron transfer from MEH-PPV to r-GO results in protecting MEH-PPV from further chemical degradation reaction. This work shows that graphene is promising as both an electron acceptor and light stabilizer for applications in optoelectronics devices.

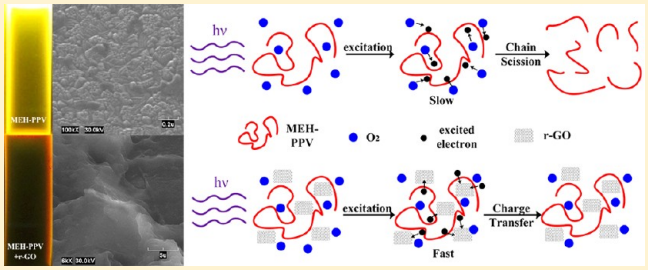

INTRODUCTION

Photoluminescence (PL) quenching has been a hot topic nowadays due to its potential application in many extensive fields of material science and biomedical applications.[1] Nanoquenchers, such as molecular beacons (MBs), are a recent example where the basic mechanism is based on PL quenching of it. Many nonconventional applications that are responsible for PL quenching have been explored, including detection of metal ions and small molecules, production of molecules (singlet oxygen), and control of DNA hybridization.[2] A variety of molecular interactions such as molecular rearrangements (static quenching), collisional quenching (dynamic quenching), energy transfer,[3] electron transfer, excited-state reactions, and self-quenching are responsible for PL quenching.

In polymer solar cells, PL quenching is a symbol of the exciton separation transfer at the interface of donor/acceptor. The polymer/fullerene derivate based donor/acceptor system is widely studied due to this efficient exciton separation and fast charge transfer at the polymer/fullerene interface.[4−7] Recently, power conversion efficiencies of up to 6.5% are achieved with the bulk heterojunction solar cells, which use the fluorescent conducting polymer poly(3-hexylthiophene) (P3HT) as the electron donor and the ICBA fullerene derivate as the acceptor.[4] The most efficient single cell polymer solar cell to date in the lab utilizes a thin layer of alcohol/water-soluble polymer as the cathode interlayer, which results in a high power conversion efficiency up to 8.37% for PCDTBT/PTB7 devices.[5] However, the electron mobility in these structures strongly depends on fullerene clustering and hopping transport.[8−10] Several groups use single-walled and multiwalled carbon nanotubes (SMCNTs and MWCNTs) as potential replacements for fullerene derivatives as the acceptor due to its unique conductivity and mechanical properties.[11,12] All of these carbon-based materials exhibit efficient quenching of the polymer PL or a faster PL decay, which indicates that photoinduced electron transfer from donor to acceptor occurred.[11−15] It is well-known that one of the essential factors for an efficient photovoltaic device is the fast and efficient transfer of photoinduced charges from donor to acceptor before photogenerated excitons recombine and decay to ground state, emitting fluorescence or heat, which results in a poor efficiency devise. Therefore, composites that show high PL quenching have priority in applications for improving performance of polymer solar cells.[16,17]

Received: July 4, 2012
Revised: September 17, 2012
Published: October 8, 2012

Graphene, as a very recent rising star in materials science with a two-dimensional (2D) structure consisting of sp^2-hybridized carbon, exhibits remarkable electronic and mechanical properties that qualify it for application in future optoelectronic devices.[18−20] A group from Cambridge developed the optoelectronic properties of graphene to realize an ultrafast laser, which harnessed the wideband optical nonlinearity of graphene with no need of band gap engineering.[21] Reduced graphene oxide (r-GO) is a promising precursor for bulk production of graphene-based materials, as it can be synthesized in large quantities and produce processable graphene nanosheets (GNs) on a large scale, which brings the advantages of low cost and large quantity production.[22] Moreover, residual functional groups on r-GO could make better contact with the polymer when their composites formed. In fact, several unique properties of graphene have motivated its investigation as a potential replacement for fullerene derivatives as the acceptor phase of devices. Recently, a study has shown that bulk heterojunction layers, consisting of graphene blended with the conjugated polymer P3HT or P3OT, can function as reasonably efficient organic photovoltaic devices.[14,15,23] Moreover, it is found that the use of graphene-enriched P3HT as a p-type polymer improves the solar cell efficiency due to the enhanced hole collection in P3HT with the presence of graphene.[24] All of these polymer/graphene based solar cells show different extents of PL quenching based on different amounts of graphene they used. However, the mechanism of this fluorescence quenching, using graphene as the electron acceptor in these studies, has not been extensively discussed. As a result, preparation of composite materials, consisting of conducting polymer donors and carbon nanomaterials as the acceptor, is an active area of research drawing enormous attention.

Despite possessing promising properties, the stability of conjugated polymers such as MEH-PPV in optoelectronic devices has always been a challenge due to the degradation of the fluorescence polymer. The main cause for this degradation is the chemical reaction origin from the effect of organic/nonaqueous solvents and dissolved molecular oxygen while processing and from the exposure to or irradiation under UV or visible sunlight.[25,26] This leads to inferior quality devices in several cases that require photostability of MEH-PPV or other similar kinds of conjugated polymeric materials.

In this paper, we report the PL quenching and photostability enhancement of MEH-PPV by introducing r-GO. The morphology of the pristine MEH-PPV, as-prepared r-GO, and MEH-PPV/r-GO composite was observed by SEM. The nature of PL quenching and enhancement of photostability of MEH-PPV by addition of r-GO was carefully studied by UV−vis spectra, PL spectrum, and transient fluorescence spectrum (TFS). In addition, the phenomenon and mechanism of improvement on the photostability of the composite have been investigated and discussed.

EXPERIMENTAL SECTION

Chemicals and Solvents. MEH-PPV used in this study was purchased from Sigma-Aldrich and used as received. GO was prepared from natural graphite (Wodetai Ltd. Co., Beijing, China, 99.9%) by a classical Hummers method with some modification.[27,28] The graphene used here was reduced from GO followed a convenient method under a low-temperature and atmosphere pressure reported elsewhere.[29] Other solvents were used directly as received without further purification. Figure 1a shows the molecular formulas of MEH-PPV and r-GO used in this study.

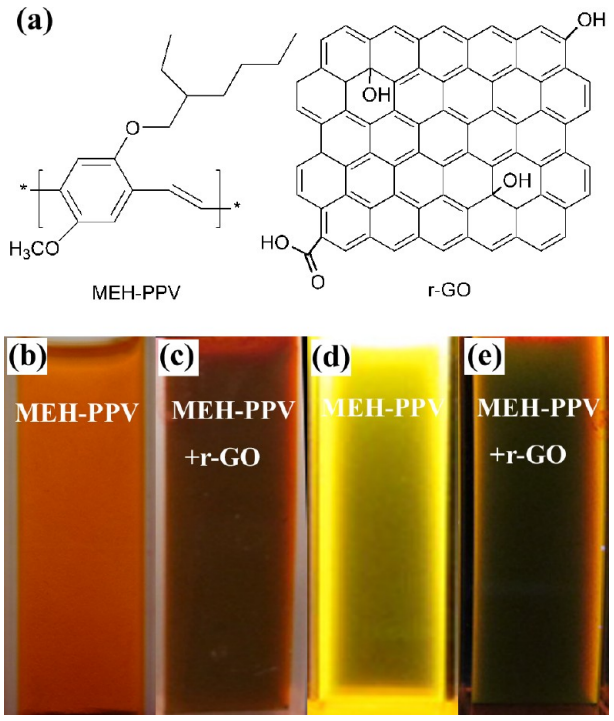

Figure 1. (a)Molecular formula of MEH-PPV and r-GO, and photograph of chloroform solution of (b) MEH-PPV under white light, (c) MEH-PPV/r-GO composite under white light, (d) MEH-PPV under 365 nm UV light, and (e) MEH-PPV/r-GO composite under 365 nm UV light.

Synthesis of Graphene Oxide (GO). In a typical synthesis, 3 g of graphite powder was put into an 80 °C solution of 12 mL of concentrated H_2SO_4, 2.5 g of $K_2S_2O_8$, and 2.5 g of P_2O_5. The mixture was kept at 80 °C for 5 h in a water bath. Successively, the mixture was cooled to room temperature, diluted with 500 mL of H_2O, and left overnight. After that, the mixture was filtered and washed with H_2O using a 0.45 μm Millipore filter to remove the residual acid. The product was dried in a vacuum oven at room temperature. This preoxidized graphite was then subjected to oxidation by Hummers' method described as follows. Preoxidized graphite powder was put into 120 mL of cold (0 °C) concentrated H_2SO_4. Then, 15 g of $KMnO_4$ was added 1 g at a time under stirring, and the temperature of the mixture was kept below 20 °C by cooling in ice. Successively, the mixture was stirred at 35 °C for 2 h and then carefully diluted with 250 mL of H_2O. After that, the mixture was stirred for another 2 h, and then an additional 700 mL of H_2O was added under stirring followed by 20 mL of 30% H_2O_2. The resulting brilliant-yellow mixture was filtered and washed with 10 wt % HCl aqueous solution (1000 mL) to remove metal ions and washed repeatedly with H_2O to remove the acid until the pH of the filtrate was neutral. The resulting GO slurry was dried in a vacuum oven at 60 °C.

Synthesis of Graphene. Graphene was thermal reduction from GO following the method reported by Chen and Yan.[29] Typically, 80 mg of the as-prepared GO were dispersed into 24 mL of water under mild ultrasound for 30 min. Then 80 mL of DMAc was added under continuous ultrasound. Finally, a transparent yellow−brown suspension of GO was obtained.

dx.doi.org/10.1021/jp306631y | J. Phys. Chem. C 2012, 116, 23053−23060

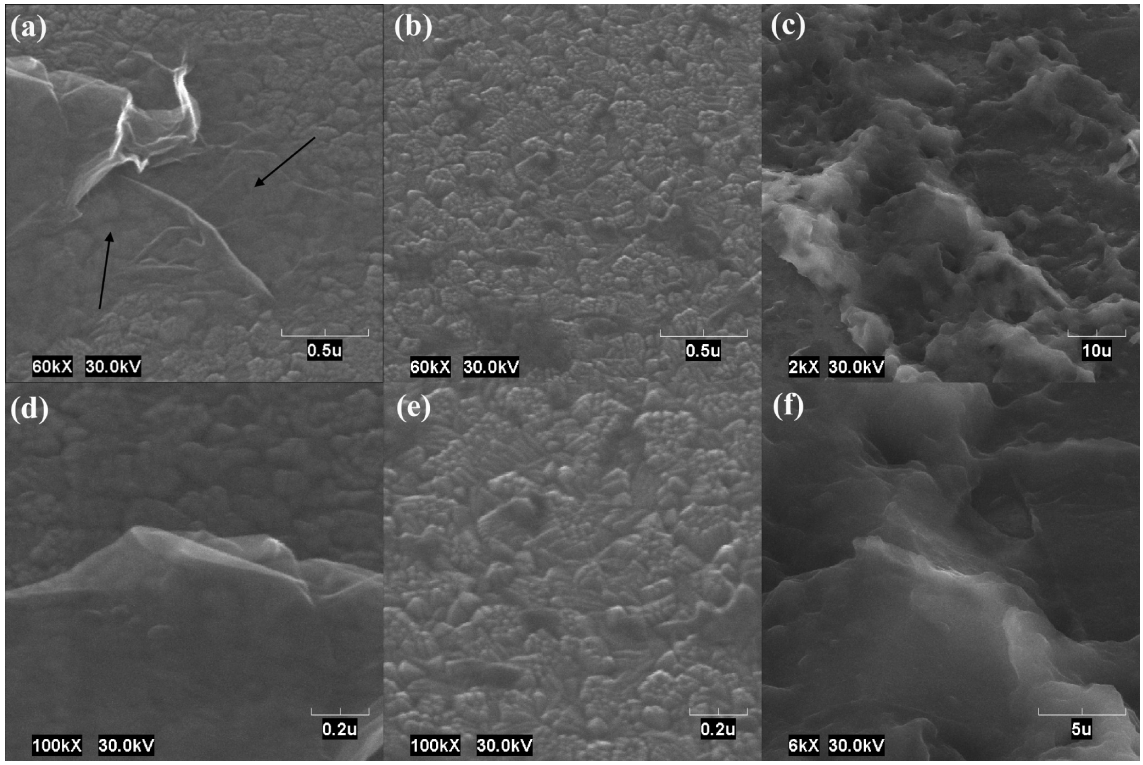

Figure 2. SEM micrographs of (a) as-prepared r-GO, (b) pristine MEH-PPV, (c) MEH-PPV/r-GO composite, and (d–f) high resolution SEM of as-prepared r-GO, pristine MEH-PPV, and MEH-PPV/r-GO composite, respectively.

After that, the suspension was loaded into a 250 mL dried three-necked flask, and nitrogen gas was bubbled through the suspension for 30 min to remove the dissolved oxygen gas, and it was heated in an oil-bath at 150 °C for 5 h under the protection of nitrogen gas. After the reaction, the suspensions were filtered through Millipore filters, and the resulting cake-like powder was washed by anhydrous ethanol three times. The powder can be redissolved in chloroform at 1 mg/mL.

Instrumentation. Scanning electron microscopic (SEM) images were recorded in CABL-9000C (CRESTEC, Japan). Ultrasonication was done in a KH300DE ultrasonicator to disperse and make uniform composites. UV–vis spectra were recorded on a Jasco V-570 UV/vis/NIR spectrophotometer at room temperature. PL studies were done using a Gilden Photonics photoluminescence spectrophotometer, and the slit widths at the excitation and the emission of the spectrofluorimeter were 5 and 2 nm, respectively. A transient fluorescence spectrum (TFS) was recorded in a FLS 920 Fluorescence Lifetime and Steady State Spectroscopy (Edinburgh Instruments, British), and samples were excited with a 369 nm diode laser (EPLED-360 ps pulsed light emitting diode, Edinburgh Instruments British). The emission was monitored at 600 nm. UV degradation experiments were performed under 365 nm UV lamp (TL-K 40 W ACTINIC BL reflector, Philips), and the intensity of the light at 365 nm is 0.978 mW/cm^2, which detected by ultraviolet radiation meter (UV-A, Beijing Normal University Photoelectric Instrument Plant) at the place where the degradation experiment was studied.

UV–visible and Photoluminescence Studies. Solutions of the MEH-PPV/r-GO composite were prepared by simple ultrasonication technique by sonicating them for 30 min. For PL and TFS studies, 2 mL of 1 mg/mL MEH-PPV chloroform solution mixed with different weight ratio of 1 mg/mL of r-GO chloroform solution, and concentrations of the pristine MEH-PPV and composites were kept the same. For the UV–vis study, necessary equivalent dilutions of both pristine MEH-PPV solution and composite solutions were made using microsyringe. UV degradation was carried out under 365 nm UV lamp in steps of 4 h exposure time, and the UV–visible and photoluminescence spectra were recorded after each exposure.

RESULTS AND DISCUSSION

Morphological Characterization of MEH-PPV, As-Prepared r-GO and MEH-PPV/r-GO Composites. Figure 1b–e shows the digital images of pristine MEH-PPV and MEH-PPV/r-GO composite under white light and UV light, respectively. It was observed that the original orange color of MEH-PPV solution turns dark brown in the composite. And under UV light, pristine MEH-PPV emitted bright yellow color while the composite became darker brown.

SEM images were recorded on dried samples on ITO glass without coating gold. Figure 2(a) depicts the SEM image of as-prepared r-GO spin-coated on ITO glass. Clearly, the rippled structure of r-GO is illustrated. Besides, it is unambiguous that ITO surface can be seen through the r-GO lamina as pointed out by arrow. These results reveal that the as-prepared graphene is in a single layer, and the obtained graphene is of the order of micrometres in size. Figure 2(b) shows the SEM image of pristine MEH-PPV film appearing as smooth and uniform thickness with micrometer size porous structure and had a filament-like shape.[30] In the case of MEH-PPV/r-GO composite, as shown in Figure 2c, wrinkle of silk-like shape of composite is uniformly distributed, indicating the formation of MEH-PPV/r-GO composite. High resolution SEM images of as-prepared r-GO, pristine MEH-PPV, and MEH-PPV/r-GO composite are shown in Figure 2d–f, respectively.

dx.doi.org/10.1021/jp306631y | J. Phys. Chem. C 2012, 116, 23053–23060

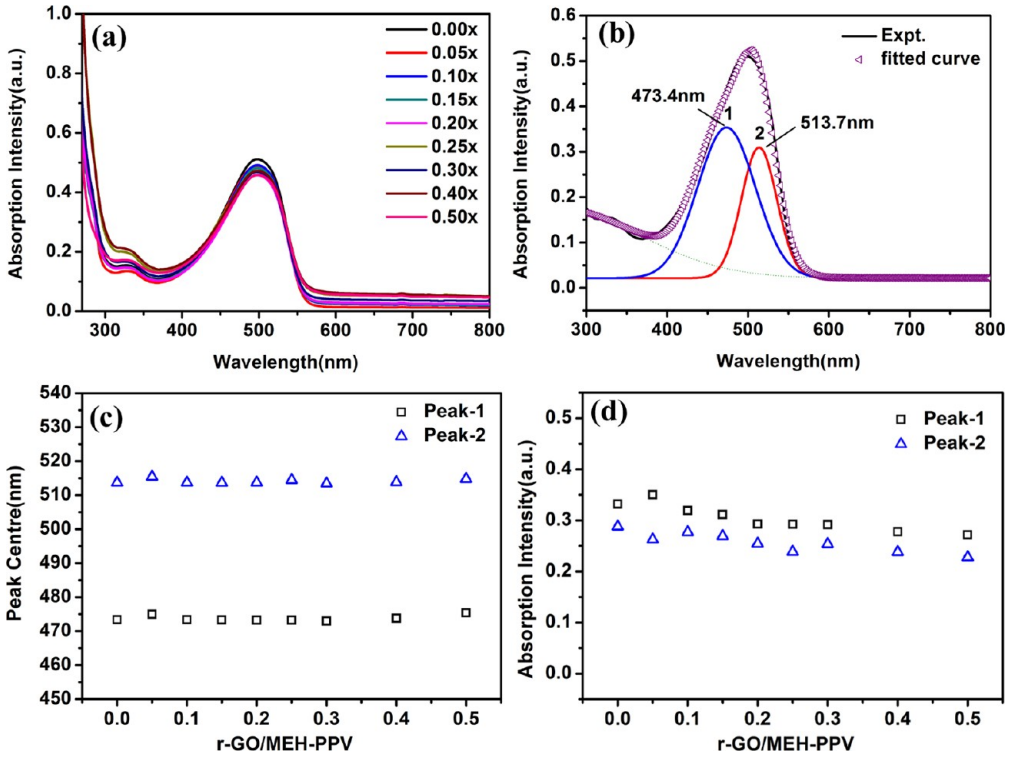

Figure 3. UV−vis spectra of (a) MEH-PPV with addition of r-GO, (b) Gaussian peak function fitted peaks, (c) change in peak center, and (d) changes in absorption intensity.

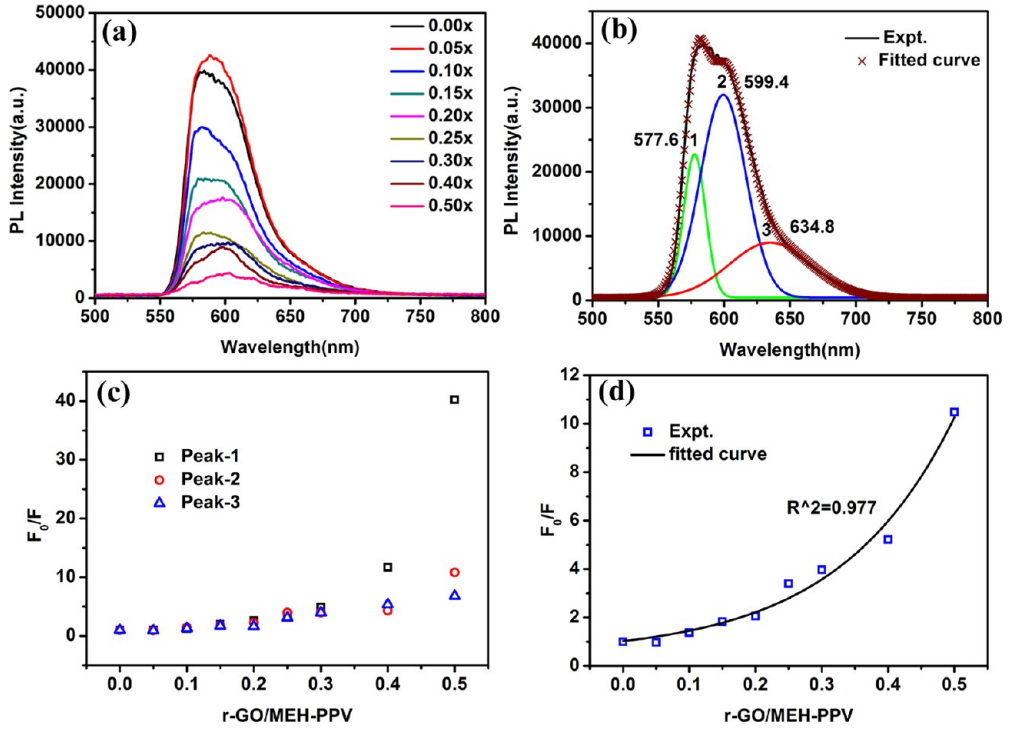

Figure 4. Photoluminescence quenching of (a) MEH-PPV with addition of r-GO, (b) Gaussian peak function fitted peaks, (c) SV plot corresponding to those three components, and (d) SV plot corresponding to the total intensity of the curve measured experimentally at integrated peak position.

UV−vis and Photoluminescence Spectroscopy. The UV−vis absorption spectra of MEH-PPV with increasing weight ratio of r-GO are shown in Figure 3a. Here, 0.00x refers to the starting weight ratio of r-GO to MEH-PPV, that is, the pristine MEH-PPV, and so on. The absorption spectrum of pristine MEH-PPV is in excellent agreement with the results reported earlier in the literature.[31] All of these measured curves are fitted with the use of a Gaussian peak function to accurately determine the area, position, line width, and intensity of each peak. Figure 3b shows the fitted curve of the MEH-PPV

dx.doi.org/10.1021/jp306631y | J. Phys. Chem. C 2012, 116, 23053−23060

solution in chloroform without additional r-GO. Clearly, the curve consists of two peaks with peak centers at 473.4 and 513.7 nm, assigned as peak-1 and peak-2, respectively. These main characteristic absorption peaks are attributed to the transition between the MEH-PPV frontier orbitals of $\pi-\pi^*$.[32] The broad absorption peak indicates that the energy gap of MEH-PPV is not equal everywhere in the molecular chain but is distributed in a small range due to the amorphous state of the polymer. Figure 3c shows the change of peak center of those curves with the increasing weight ratio of r-GO to MEH-PPV. It is conspicuous that little offset in the peak center of absorption spectra appears with the addition of r-GO. This result indicates that the existence of r-GO hardly influences the structure of MEH-PPV; in other words, the molecular interaction between the two materials is weak though the MEH-PPV/r-GO composite is indeed formed. As we all know, graphene can be repeatedly peeled from graphite by micromechanical exfoliation due to the weak interaction between each layer. Therefore, the born nature of the weak interaction of graphene makes a reasonable explanation,[18,19] and this weak interaction also reflects the well-reduction of the graphene as shown in the SEM images. The change in intensity of the two peaks with the increasing ratio of r-GO is shown in Figure 3d. Both peak-1 and peak-2 do not show appreciable change in absorption intensity, which also indicates that the addition of r-GO has little influence on the light absorption of MEH-PPV. A similar phenomenon is observed in the composite of P3HT-SWCNT, which shows no change in absorption spectra as well due to the weak interaction between the luminescence polymer and SWCNT.[12,13]

Figure 4a shows a decrease in the PL spectra of composites with increasing ratio of r-GO/MEH-PPV, which indicates a significant fluorescence quenching of the composites. It is noteworthy that at low ratio (less than 0.05x) the fluorescence of the composite is not quenched but rather enhanced. One reasonable explanation is that the small quantity of r-GO in dispersion might lead to more effective scattering of the emitted light, thereby enhancing the MEH-PPV fluorescence.[3] In order to investigate the quenching efficiency and mechanism of PL quenching of r-GO for MEH-PPV, all of these PL spectra were also fitted using a Gaussian peak function. Figure 4b shows the fitted curve of pristine MEH-PPV, which is found to consist with three peaks at wavelengths of 577.6, 599.4, and 634.8 nm, assigned as peak-1, peak-2, and peak-3, respectively. The origin of these fluorescent peaks lies in the relaxation process of the excited electrons from the excited state back to the ground state in the MEH-PPV molecule. The different positions of absorption peaks (around 500 nm) and fluorescent peaks (around 600 nm) are mainly caused by energy loss through molecular collision and solvent relaxation, resulting in this red shift of the emission peak. The Stern−Volmer (SV) plot corresponding to those three components is shown in Figure 4c. Figure 4d shows the SV plot corresponding to the total intensity of the curve measured experimentally at integrated peak position. The SV plot is defined as the ratio of the fluorescence intensity without graphene (F_0) to the intensity with graphene (F) as a function of graphene weight ratio. In Figure 4c, when the weight ratio of r-GO is less than 0.20X, the SV plots of all three peaks are fully linear, which suggests that there is only one species, namely quencher A, taking effect here and leads to a linear quenching process. However, when addition of r-GO is over 0.20X, it gradually shows an exponential increase of quenching, which indicates that there is another quencher or more starting to work in the system and they are more effective at quenching than quencher A. Because if not, the SV plot at high r-GO concentration should remain linear with the addition of r-GO. As a result, more than one species may be involved simultaneously in the quenching process when the weight ratio of r-GO is more than 0.20X. Unfortunately, what the exact species is that causes this exponential increase in PL quenching at a high ratio of r-GO (>0.20X) is still ambiguous. One possible reason is that, at higher concentration, the newcomer r-GO results in locality overlay of r-GO due to the attractive van derWaals forces among nanoscale graphene holding the graphene sheets together.[33] This may lead to the partial presence of multilayer graphene, whose quenching ability is better and results in a nonlinear SV plot. Besides, at 0.50x weight ratio of r-GO to MEH-PPV, the SV plot presents a high value of F_0/F, corresponding to a reduction in fluorescence intensity of more than 90%.

Furthermore, the possibility of the existence of energy transfer (also known as fluorescence resonance energy transfer (FRET)), which occurs at certain distances through energy exchange between radiating dipoles due to long-range dipole−dipole interactions,[34] is eliminated. Two points have to be achieved to make FRET happen: (i) the distance between the donor and acceptor should be no more than 10 nm and (ii) there must be an overlap between the donor's fluorescence spectrum and the acceptor's absorption spectrum so that the energy emitted by the donor could be received and absorbed by the acceptor through resonance.[35] In our case, there is no overlap between the fluorescence spectrum of MEH-PPV and the absorption spectrum of r-GO as shown in Figure 5, which

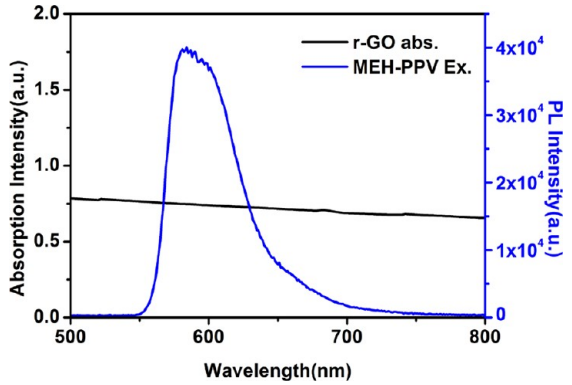

Figure 5. Photoluminescence spectrum of MEH-PPV and absorption spectrum of r-GO showing no overlap and indicating that electron transfer rather than energy transfer happens at the interface of the composite.

indicates that electron transfer occurred at the contact surface of the composite. As a result, efficient electron transfer is confirmed which makes r-GO a favorable electron acceptor material, and this efficient electron transfer may play a crucial role in the photostability of the MEH-PPV/r-GO composite, which will be discussed later. A similar phenomenon of photoinduced electron transfer from the excited state of MEH-PPV onto C_{60} is reported in earlier in the literature where $\pi-\pi$ interactions dominate.[36]

In order to investigate the nature of the quenching process in the composite, the fluorescence lifetime, which is a visual approach to determine the type of quenching, was investigated.

dx.doi.org/10.1021/jp306631y | J. Phys. Chem. C 2012, 116, 23053−23060

The transient fluorescence spectrum (TFS) of composites with increasing weight ratio of r-GO/MEH-PPV in solution is shown in Figure 6a. Samples were measured at room temperature. It clearly shows that all of these spectra overlapped with each other with continuous addition of r-GO. Then, these spectra were deconvoluted using exponential decay profile to estimate the PL lifetime. Figure 6b shows TFS of pristine MEH-PPV which indicates two decay times with 0.47 ns (τ_1) and 3.28 ns (τ_2) responsible for 14.16% and 84.88% of the decay process, respectively. Figure 6c shows the variation in τ_0/τ for the decay times τ_1 and τ_2 with increasing addition of r-GO. Obviously, τ_0/τ for both decay times τ_1 and τ_2 with increasing r-GO remains nearly constant at 1. This result eliminates the possibility of dynamic quenching in these composites, since a decrease in fluorescence lifetime would be observed in such a quenching process. This is consistent with SEM observed above, which shows the formation of the MEH-PPV/r-GO composite. Therefore, static quenching is confirmed in the MEH-PPV/r-GO composite, for the presence of r-GO has no effect on the fluorescence lifetime of MEH-PPV. Similar results are also obtained in P3HT/MWCNT and P3HT/SWCNT composites,[12] indicating that these kinds of nanocarbon materials, which exhibit unique photoluminescence quenching ability, are appropriate candidates for the electron acceptor of photovoltaic devices.

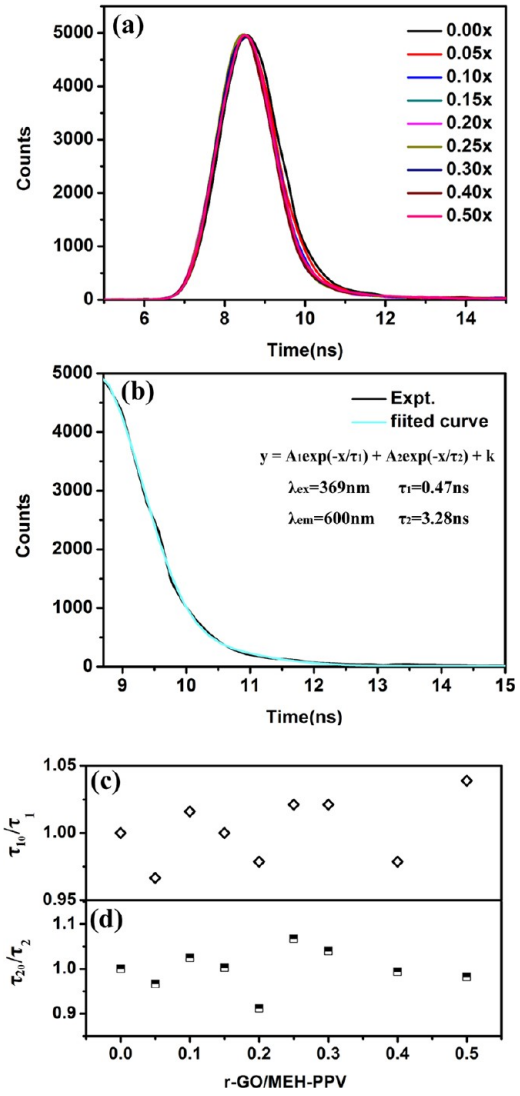

Figure 6. Transient fluorescence spectrum (TFS) of MEH-PPV with addition of r-GO (a), showing two exponential decay times τ_1 = 0.47 ns and τ_2 = 3.28 ns (b). Variation in the relative decay lifetime of τ_1 and τ_2 components with addition of r-GO shows a nearly constant value of 1 representing static quenching (c).

Further, the photostability enhancement of the r-GO -covered MEH-PPV composite has been studied. In photovoltaic devices, photostability is one of the most crucial factors that determine the performance and lifetime of devices.[37] To study the photodegradation behavior, MEH-PPV loaded with and without r-GO was exposed to UV radiation in chloroform solution in 4 h steps of irradiation time. Here, we choose the high r-GO concentration of 0.50X, which shows almost complete PL quenching of MEH-PPV. With continuous UV irradiation on the chloroform solution of pristine MEH-PPV, a rapid decrease in absorption intensity and significant blue shifts (from 498 to 400 nm) after 16 h of radiation were observed as shown in Figure 7a. In conjugated polymers, the degree of polymerization directly affects the $\pi-\pi^*$ transition in the polymer molecular which appears as the maximum absorption peak.[38] Thus, this process indicates that the $\pi-\pi$ conjugated system is broken and the MEH-PPV molecular chain is ruptured due to the coefficient of photoinduced exciton and O_2, which will be discussed later. However, in the case of MEH-PPV/r-GO composite shown in Figure 7b, it shows no change in the characteristic absorption peak after 12 h of UV radiation. After 16 h of UV exposure, a negligible 8 nm blue shift of the maximum absorption peak with a small decrease in the absorption intensity was observed. Observations from these absorption spectra under UV irradiation are evidence that directly shows effective enhancement on the photostability of the luminescence polymer MEH-PPV by r-GO, which protects it from photodegradation under UV light due to the fast exiton transfer. This may improve the performance and lifetime of photovoltaic devices.

The PL spectra of MEH-PPV and the MEH-PPV/r-GO composite exposed to UV light are shown in Figure 7, panels c and d, respectively. Clearly, pristine MEH-PPV shows a significant PL quenching after continuous UV radiation, which indicates that degradation of the polymer occurred after 16 h of exposure to UV irradiation. In the case of the MEH-PPV/r-GO sample, there is no further decrease in intensity or peak shift with continuous UV irradiation after 16 h, indicating the markedly enhancement on the photostability of the composite. This is consistent with the UV−vis spectra discussed above. This PL result, together with absorption spectra of MEH-PPV and the MEH-PPV/r-GO composite exposed to UV light, represents the unique photostabilities of r-GO on MEH-PPV and probably other kinds of fluorescent conjugated polymers.

Mechanism of Photodegradation of MEH-PPV in Solution. At last, we discuss the mechanism of photodegradation of MEH-PPV and the photostability of MEH-PPV by r-GO. The photodegradation of polymers has been well studied earlier in the literature.[39−41] It is found that, in pure polymer, the presence of UV light and molecular oxygen could lead to gradual degradation of the fluorescent polymer, which results in photobleaching. The reaction that occurred here is shown in Scheme 1.[39] Oxygen was shown to initially favor its formation by photoinduced electron transfer leading to the formation of the superoxide anion $O_2^{\bullet-}$.[32] The charged radicals

dx.doi.org/10.1021/jp306631y | J. Phys. Chem. C 2012, 116, 23053−23060

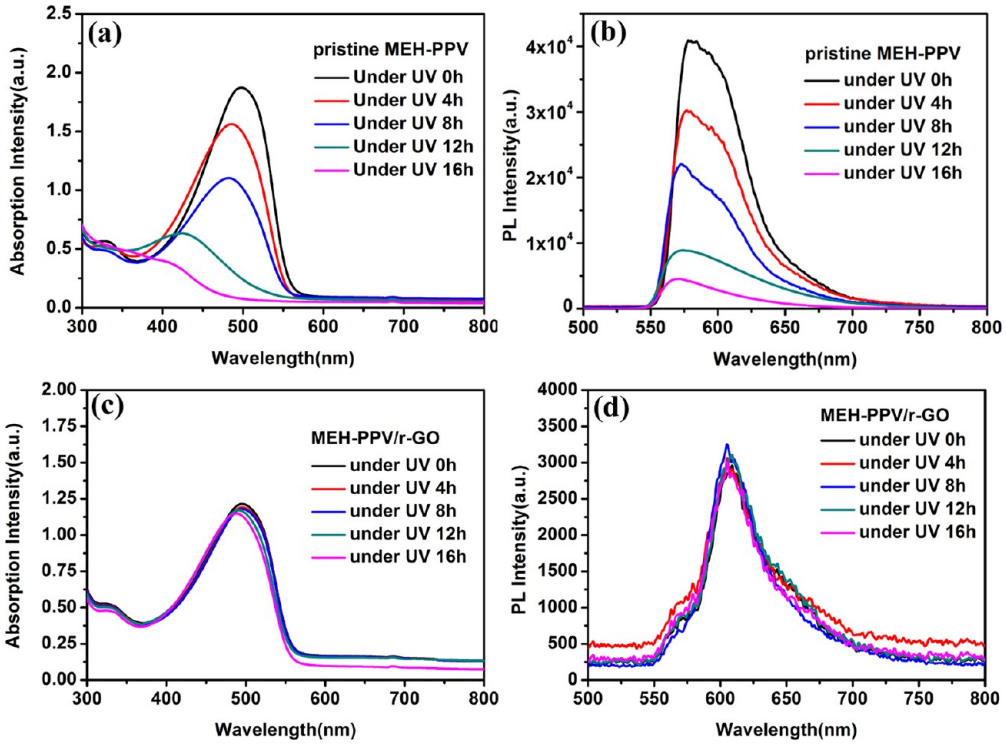

Figure 7. UV−vis absorption (a) and photoluminescence spectra (b) of MEH-PPV after 16 h of UV exposure and UV−vis absorption (c) and photoluminescence spectra (d) of MEH-PPV/r-GO composite after 16 h of UV exposure.

Scheme 1. Photodegradation Reaction of MEH-PPV

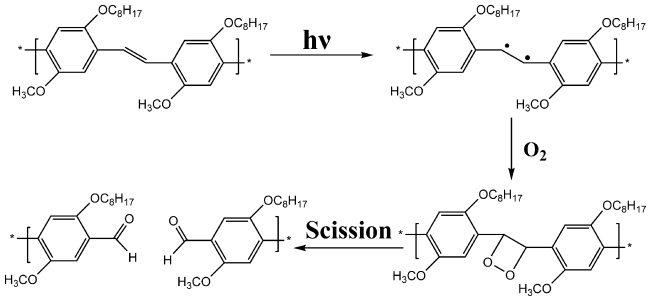

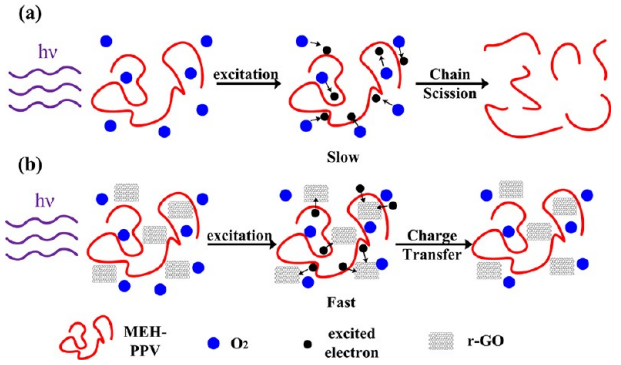

Figure 8. Mechanism of (a) photodegradation of MEH-PPV and (b) MEH-PPV protected by r-GO; note that the polymer molecular is protected by r-GO due to fast electron transfer at the interface of the two materials.

are likely to evolve by oxidation and scission of the polymer molecule, and the resulting radicals propagate the chain oxidation process by abstraction of the labile hydrogen atom of the polymer.[39] Although this process can proceed slowly, it still limits the stability of the fluorescence polymer to some extent. This finally leads to chain scission of the polymer which no longer shows emission fluorescence as shown in Figure 8a and thus shortens the lifetime of photovoltaic devices. However, in the case of the MEH-PPV/r-GO composite, as shown in Figure 8b, the excited electron in MEH-PPV transfers rapidly onto r-GO due to the efficient electron transfer at the interface of the two materials. This process cuts off the channel that forms the superoxide anion $O_2^{\bullet-}$ described above, and the following degradation reaction will not occur. Therefore, the polymer is well protected and can maintain and function for a relatively long period of time.

CONCLUSION

Nanocomposites of MEH-PPV polymer and r-GO were prepared by an ultrasonication technique, which is a convenient and easy method of preparing uniform composites from readily available polymeric materials and graphene. We have observed that MEH-PPV and r-GO form a homogeneous composite, and efficient PL quenching occurred with the existence of r-GO. From transient fluorescence spectra, the nature of this PL quenching observed in the MEH-PPV/r-GO composite is confirmed to be static quenching, and more than one species is involved simultaneously in the quenching process when the weight ratio of r-GO is more than 0.20X. In addition, electron transfer rather than energy transfer is confirmed because there is no overlap between the fluorescence spectrum of MEH-PPV and the absorption spectrum of r-GO. Furthermore, we propose that this very fast electron transfer results in the enhancement of the photochemical stability of the fluorescence polymer, since this process avoids the oxidation and scission of the polymer molecular. This study provides potential applications of graphene as both electron acceptor and light

dx.doi.org/10.1021/jp306631y | J. Phys. Chem. C 2012, 116, 23053−23060

stabilizer in optoelectronics and polymer-based photovoltaic devices.

AUTHOR INFORMATION

Notes

The authors declare no competing financial interest.

ACKNOWLEDGMENTS

The authors gratefully acknowledge financial support from Natural Science Foundation of China (Grant Nos. 91123019, 61176056, and 61177059). This work has been financially supported by the Key Project of Basic Science Research of Shaanxi Province (2009JZ2015), the "13115" Innovation Engineering of Shaanxi Province (2010ZDKG-58), and the open projects from the Institute of Photonics and Photo-Technology, Provincial Key Laboratory of Photoelectronic Technology, Northwest University, China.

REFERENCES

(1) Anni, M.; Rella, R. *J. Phys. Chem. B* **2010**, *114*, 1559−1561.
(2) Huang, K.; Angel, A. M. *Anal. Bioanal. Chem* **2012**, *402*, 3091−3102.
(3) Ahmad, A.; Kern, K.; Balasubramanian, K. *ChemPhysChem.* **2009**, *10*, 905−909.
(4) Zhao, G.; He, Y.; Li, Y. *Adv. Mater.* **2010**, *22*, 4355−4358.
(5) He, Z.; Zhong, C.; Huang, X.; Wong, W. Y.; Wu, H. B.; Chen, L.; Su, S.; Cao, Y. *Adv. Mater.* **2011**, *23*, 4636−4643.
(6) Brabec, C. J.; Sariciftci, N. S.; Hummelen, J. C. *Adv. Funct. Mater.* **2001**, *11*, 15−26.
(7) Yu, G.; Gao, J.; Hummelen, J. C.; Wudl, F.; Heeger, A. J. *Science* **1995**, *270*, 1789−1790.
(8) Liang, Y.; Xu, Z.; Xia, J.; Tsai, S. T.; Wu, Y.; Li, G.; Ray, C.; Yu, L. *Adv. Mater.* **2010**, *22*, E135−E138.
(9) Green, M. A.; Emery, K.; Hishikawa, Y.; Warta, W. *Prog. Photovolt.: Res. Appl.* **2010**, *18*, 346−352.
(10) Grzegorczyk, W. J.; Savenije, T. J.; Dykstra, T. E.; Piris, J.; Schins, J. M.; Siebbeles, L. D. *J. Phys. Chem. C* **2010**, *114*, 5182−5186.
(11) Sgobba, V.; Guldi, D. M. *J. Mater. Chem.* **2008**, *18*, 153−157.
(12) Goutam, P. J.; Singh, D. K.; Iyer, P. K. *J. Phys. Chem. C* **2012**, *116*, 8196−8201.
(13) Ferguson, A. J.; Blackburn, J. L.; Holt, J. M.; Kopidakis, N.; Tenent, R. C.; Barnes, T. M.; Heben, M, J.; Rumbles, G. *J. Phys. Chem. Lett.* **2010**, *1*, 2406−2411.
(14) Liu, Z.; Liu, Q.; Huang, Y.; Ma, Y.; Yin, S.; Zhang, X.; Sun, W.; Chen, Y. *Adv. Mater.* **2008**, *20*, 3924−3930.
(15) Liu, Q.; Liu, Z.; Zhang, X.; Yang, L.; Zhang, N.; Pan, G.; Yin, S.; Chen, Y.; Wei, J. *Adv. Funct. Mater.* **2009**, *19*, 894−904.
(16) Wong, W. Y.; Zhuwang, X.; He, Z.; Djuri, A. B.; Yip, C. T.; Cheung, K. Y.; Wang, H.; Mak, C. S. K.; Chan, W. K. *Nat. Mater.* **2007**, *6*, 521−527.
(17) Kuila, B. K.; Park, K.; Dai, L. *Macromolecules* **2010**, *43*, 6699−6705.
(18) Rao, C. N. R.; Sood, A. K.; Subrahmanyam, K. S.; Govindaraj, A. *Angew. Chem., Int. Ed.* **2009**, *48*, 7752−7777.
(19) Tang, L.; Wang, Y.; Li, Y.; Feng, H.; Lu, J.; Li, J. *Adv. Funct. Mater.* **2009**, *19*, 2782−2789.
(20) Bonaccorso, F.; Sun, Z.; Hasan, T.; Ferrari, A. C. *Nat. Photonics* **2010**, *4*, 611−622.
(21) Sun, Z.; Hasan, T.; Torrisi, F.; Popa, D.; Privitera, G.; Wang, F.; Bonaccorso, F.; Basko, D. M.; Ferrari, A. C. *ACS Nano* **2010**, *4*, 803−810.
(22) Li, D.; Müller, M. B.; Gilje, S.; Kaner, R. B.; Wallace, G. G. *Nat. Nanotechnol.* **2008**, *3*, 101−105.
(23) Wang, Y.; Kurunthu, D.; Scott, G. W.; Bardeen., C. J. *J. Phys. Chem. C* **2010**, *114*, 4153−4159.
(24) AbdulAlmohsin, S.; Cui, J. B. *J. Phys. Chem. C* **2012**, *116*, 9433−9438.
(25) Holdcroft, S. *Macromolecules* **1991**, *24*, 4834−4838.
(26) Abdou, M. S. A.; Holdcroft, S. *Macromolecules* **1993**, *26*, 2954.
(27) Hummers, W. S. J.; Offema, R. E. *J. Am. Chem. Soc.* **1958**, *80*, 1339.
(28) Tai, Z.; Ma, H.; Liu, B.; Yan, X.; Xue, Q. *Colloids Surf., B* **2011**, *89*, 147−151.
(29) Chen, W.; Yan, L. *Nanoscale* **2010**, *2*, 559−563.
(30) Beji, L.; Jomaa, T. B.; Ltaeif, A.; Bouazizi, A. *Phys. Status Solidi A* **2005**, *202*, 1763−1767.
(31) Atreya, M.; Li, S.; Kang, E. T.; Neoh, K. G.; Ma, Z. H.; Tan, K. L.; Huang, W. *Polym. Degrad. Stab.* **1999**, *65*, 287−296.
(32) Bronze-Uhle, E. S.; Batagin-Neto, A.; Lavarda, F. C.; Graeff, C. F. O. *J. Appl. Phys.* **2011**, *110*, 073510.
(33) Das, S.; Wajid, A. S.; Shelburne, J. L.; Liao, Y. C.; Green, M. J. *Appl. Mater. Interfaces* **2011**, *3*, 1844−1851.
(34) Berney, C.; Danuser, G. *Biophys. J.* **2003**, *84*, 3992−4010.
(35) Asbahi, B. A. A.; Alsalhi, M. S.; Dwayyan, A. S. A.; Jumali, M. H. H. *J. Lumin.* **2012**, *132*, 386−390.
(36) Sariciftci, N. S.; Smilowitz, L.; Heeger, A. J.; Wudl, F. *Science* **1992**, *258*, 1474.
(37) Wang, Y.; Wei, W.; Liu, X.; Gu, Y. *Solar Energy Mater. Solar Cells* **2012**, *98*, 129−145.
(38) Goutam, P. J.; Singh, D. K.; Giri, P. K.; Iyer, P. K. *J. Phys. Chem. B* **2011**, *115*, 919−924.
(39) Scurlock, R. D.; Wang, B.; Ogilby, P. R.; Sheats, J. R.; Clough, R. L. *J. Am. Chem. Soc.* **1995**, *117*, 10194−10202.
(40) Yan, M.; Rothberg, L. J.; Papadimitrakopoulos, F.; Galvin, M. E.; Miller, T. M. *Phys. Rev. Lett.* **1994**, *73*, 744−747.
(41) Papadimitrakopoulos, F.; Yan, M.; Rothberg, L. J.; Katz, H. E.; Chandross, E. A.; Galvin, M. E. *Mol. Cryst. Liq. Cryst.* **1994**, *256*, 663−669.